Composite Structures 94 (2012) 1814–1825

Contents lists available at SciVerse ScienceDirect

Composite Structures

journal homepage: www.elsevier.com/locate/compstruct

A quasi-3D hyperbolic shear deformation theory for the static and free vibration analysis of functionally graded plates

A.M.A. Neves [a], A.J.M. Ferreira [a,*], E. Carrera [c], M. Cinefra [c], C.M.C. Roque [b], R.M.N. Jorge [a], C.M.M. Soares [d]

[a] Departamento de Engenharia Mecânica, Faculdade de Engenharia, Universidade do Porto, Rua Dr. Roberto Frias, 4200-465 Porto, Portugal
[b] INEGI, Faculdade de Engenharia, Universidade do Porto, Rua Dr. Roberto Frias, 4200-465 Porto, Portugal
[c] Departament of Aeronautics and Aerospace Engineering, Politecnico di Torino, Corso Duca degli Abruzzi, 24, 10129 Torino, Italy
[d] Instituto Superior Técnico, Technical University of Lisbon, Av. Rovisco Pais, 1049-001 Lisboa, Portugal

ARTICLE INFO

Article history:
Available online 29 December 2011

Keywords:
Functionally graded materials
Meshless methods
Plates and shells

ABSTRACT

This paper presents an original hyperbolic sine shear deformation theory for the bending and free vibration analysis of functionally graded plates. The theory accounts for through-the-thickness deformations.

Equations of motion and boundary conditions are obtained using Carrera's Unified Formulation and further interpolated by collocation with radial basis functions.

The efficiency of the present approach combining the new theory with this meshless technique is demonstrated in several numerical examples, for the static and free vibration analysis of functionally graded plates. Excellent agreement for simply-supported plates with other literature results has been found.

1. Introduction

Functionally graded materials (FGM) are a class of composites in which the properties change gradually over one or more directions. A typical FGM plate presents a continuous variation of material properties over the thickness direction by mixing two different materials [1]. The gradual variation of properties avoids the delamination failure that is common in laminated composites.

Typically, the analysis of FGM plates is performed using the first-order shear deformation theory (FSDT) [2–5] or higher-order shear deformation theories (HSDT) [3,5–8]. The FSDT gives acceptable results but depends on a shear correction factor which is difficult to find as it depends on many parameters. There is no need of a shear correction factor when using a HSDT but equations of motion are more complicated to obtain than those of the FSDT.

Typically functionally graded plates have been analysed with shear deformation theories that neglect the thickness stretching ϵ_{zz}, considering the transverse displacement independent of the thickness coordinate. The effect of thickness stretching in FGM plates has been recently investigated by Carrera et al. [9], using finite element approximations.

The use of alternative methods to the Finite Element Methods for the analysis of plates, such as the meshless methods based on collocation with radial basis functions (RBFs) is atractive due to the absence of a mesh and the ease of collocation methods. In recent years, radial basis functions showed excellent accuracy in the interpolation of data and functions. Kansa [10] introduced the concept of solving partial differential equations by an unsymmetric RBF collocation method based upon the multiquadric interpolation functions. The authors have recently applied the RBF collocation to the static deformations and free vibrations of composite beams and plates [11–18].

The present paper addresses the thickness stretching effect on the static and free vibration analysis of FGM plates, by a meshless technique based on collocation with radial basis functions. The Unified Formulation proposed by Carrera (further denoted as CUF) method [19,20] is employed to obtain the algebraic equations of motion and boundary conditions. Such equations of motion and corresponding boundary conditions are then interpolated by radial basis functions to obtain an algebraic system of equations. The CUF method has been applied in several finite element analysis, either using the Principle of Virtual Displacements, or by using the Reissner's Mixed Variational theorem. The stiffness matrix components, the external force terms or the inertia terms can be obtained directly with this unified formulation, irrespective of the shear deformation theory being considered.

To the best of authors' knowledge, plate theories involving hyperbolic functions are quite rare in literature. Soldatos [21] used a displacement field involving the hyperbolic function

$$f(z) = h\sinh\left(\frac{z}{h}\right) - z\cosh\left(\frac{1}{2}\right). \tag{1}$$

* Corresponding author.
E-mail address: ferreira@fe.up.pt (A.J.M. Ferreira).

0263-8223/$ - see front matter © 2011 Elsevier Ltd. All rights reserved.
doi:10.1016/j.compstruct.2011.12.005

In [22,23] two displacement fields are presented both considering a hyperbolic function:

$$f(z) = \frac{3\pi}{2} h \tanh\left(\frac{z}{h}\right) - \frac{3\pi}{2} z \operatorname{sech}^2\left(\frac{1}{2}\right) \tag{2}$$

and

$$f(z) = z \operatorname{sech}\left(\frac{\pi z^2}{h^2}\right) - z \operatorname{sech}\left(\frac{\pi}{4}\right)\left[1 - \frac{\pi}{2}\tanh\left(\frac{\pi}{4}\right)\right]. \tag{3}$$

In [24] the considered hyperbolic function is

$$f(z) = \frac{\frac{h}{\pi}\sinh\left(\frac{\pi z}{h}\right) - z}{\cosh\left(\frac{\pi}{2}\right) - 1}. \tag{4}$$

In all cases the hyperbolic functions are used for the in-plane expansions only, while the transverse displacement is kept constant ($w = w_0$).

The use of hyperbolic shear deformation theory accounting for $\epsilon_{zz} \neq 0$ for the static and free vibration analysis of plates has not been done yet. In this paper an hybrid quasi-3D hyperbolic shear deformation theory, with different expansion for the in-plane and the out-of-plane displacement is proposed. In-plane displacements are considered to be of hyperbolic sine type across the thickness coordinate and the out-of-plane displacement is defined as quadratic in the thickness direction. The present formulation can be seen as a enhancement of the original CUF in the sense that different displacement fields for in-plane and out-of-plane displacements are introduced.

2. Governing equations and boundary conditions

A rectangular plate of in-plane dimensions a and b and uniform thickness h is considered. The co-ordinate system is such that the x–y plane coincides with the midplane of the plate. The plate is made of a material graded across the thickness direction.

2.1. Displacement field

The following displacement field is assumed:

$$u(x,y,z,t) = u_0(x,y,t) + z u_1(x,y,t) + \sinh\left(\frac{\pi z}{h}\right) u_Z(x,y,t) \tag{5}$$

$$v(x,y,z,t) = v_0(x,y,t) + z v_1(x,y,t) + \sinh\left(\frac{\pi z}{h}\right) v_Z(x,y,t) \tag{6}$$

$$w(x,y,z,t) = w_0(x,y,t) + z w_1(x,y,t) + z^2 w_2(x,y,t) \tag{7}$$

where u, v, and w are the displacements in the x-, y-, and z-directions, respectively. u_0, u_1, u_Z, v_0, v_1, v_Z, w_0, w_1, and w_2 are functions to be determined.

2.2. Strains

The strain–displacement relationships are:

$$\left\{\begin{matrix}\epsilon_{xx}\\ \epsilon_{yy}\\ \gamma_{xy}\end{matrix}\right\} = \left\{\begin{matrix}\frac{\partial u}{\partial x}\\ \frac{\partial v}{\partial y}\\ \frac{\partial u}{\partial y} + \frac{\partial v}{\partial x}\end{matrix}\right\}, \quad \left\{\begin{matrix}\gamma_{xz}\\ \gamma_{yz}\\ \epsilon_{zz}\end{matrix}\right\} = \left\{\begin{matrix}\frac{\partial u}{\partial z} + \frac{\partial w}{\partial x}\\ \frac{\partial v}{\partial z} + \frac{\partial w}{\partial y}\\ \frac{\partial w}{\partial z}\end{matrix}\right\} \tag{8}$$

By substitution of the displacement field in (8), the strains are obtained in terms of the proposed model unknowns:

$$\left\{\begin{matrix}\epsilon_{xx}\\ \epsilon_{yy}\\ \gamma_{xy}\end{matrix}\right\} = \left\{\begin{matrix}\frac{\partial u_0}{\partial x}\\ \frac{\partial v_0}{\partial y}\\ \frac{\partial u_0}{\partial y} + \frac{\partial v_0}{\partial x}\end{matrix}\right\} + z\left\{\begin{matrix}\frac{\partial u_1}{\partial x}\\ \frac{\partial v_1}{\partial y}\\ \frac{\partial u_1}{\partial y} + \frac{\partial v_1}{\partial x}\end{matrix}\right\} + \sinh\left(\frac{\pi z}{h}\right)\left\{\begin{matrix}\frac{\partial u_Z}{\partial x}\\ \frac{\partial v_Z}{\partial y}\\ \frac{\partial u_Z}{\partial y} + \frac{\partial v_Z}{\partial x}\end{matrix}\right\} \tag{9}$$

$$\left\{\begin{matrix}\gamma_{xz}\\ \gamma_{yz}\end{matrix}\right\} = \left\{\begin{matrix}u_1\\ v_1\end{matrix}\right\} + \cosh\left(\frac{\pi z}{h}\right)\frac{\pi}{h}\left\{\begin{matrix}u_Z\\ v_Z\end{matrix}\right\} + \left\{\begin{matrix}\frac{\partial w_0}{\partial x}\\ \frac{\partial w_0}{\partial y}\end{matrix}\right\} + z\left\{\begin{matrix}\frac{\partial w_1}{\partial x}\\ \frac{\partial w_1}{\partial y}\end{matrix}\right\} + z^2\left\{\begin{matrix}\frac{\partial w_2}{\partial x}\\ \frac{\partial w_2}{\partial y}\end{matrix}\right\} \tag{10}$$

$$\epsilon_{zz} = w_1 + 2 z w_2 \tag{11}$$

2.3. Elastic stress–strain relations

The elastic stress–strain relations depends on which assumption of ϵ_{zz} we consider. If $\epsilon_{zz} \neq 0$, i.e., thickness stretching is allowed, then the 3D model is used and the constitutive equations can be written as:

$$\left\{\begin{matrix}\sigma_{xx}\\ \sigma_{yy}\\ \tau_{xy}\\ \tau_{xz}\\ \tau_{yz}\\ \sigma_{zz}\end{matrix}\right\} = \left\{\begin{matrix}C_{11} & C_{12} & 0 & 0 & 0 & C_{13}\\ C_{12} & C_{22} & 0 & 0 & 0 & C_{23}\\ 0 & 0 & C_{66} & 0 & 0 & 0\\ 0 & 0 & 0 & C_{55} & 0 & 0\\ 0 & 0 & 0 & 0 & C_{44} & 0\\ C_{13} & C_{23} & 0 & 0 & 0 & C_{33}\end{matrix}\right\}\left\{\begin{matrix}\epsilon_{xx}\\ \epsilon_{yy}\\ \gamma_{xy}\\ \gamma_{xz}\\ \gamma_{yz}\\ \epsilon_{zz}\end{matrix}\right\} \tag{12}$$

The C_{ij} are the three-dimensional elastic constants, given by

$$C_{11} = \frac{E(1-\nu^2)}{1-3\nu^2-2\nu^3}, \quad C_{12} = \frac{E(\nu+\nu^2)}{1-3\nu^2-2\nu^3}, \quad C_{22} = \frac{E(1-\nu^2)}{1-3\nu^2-2\nu^3},$$

$$C_{13} = \frac{E(\nu+\nu^2)}{1-3\nu^2-2\nu^3}, \quad C_{23} = \frac{E(\nu+\nu^2)}{1-3\nu^2-2\nu^3}, \tag{14}$$

$$C_{44} = G, \quad C_{55} = G, \quad C_{66} = G, \quad C_{33} = \frac{E(1-\nu^2)}{1-3\nu^2-2\nu^3} \tag{15}$$

where E is the modulus of elasticity, ν is Poisson's ratio, and G is the shear modulus $G = \frac{E}{2(1+\nu)}$.

If $\epsilon_{zz} = 0$, then the plane-stress case is used

$$\left\{\begin{matrix}\sigma_{xx}\\ \sigma_{yy}\\ \tau_{xy}\\ \tau_{xz}\\ \tau_{yz}\end{matrix}\right\} = \left\{\begin{matrix}C_{11} & C_{12} & 0 & 0 & 0\\ C_{12} & C_{22} & 0 & 0 & 0\\ 0 & 0 & C_{66} & 0 & 0\\ 0 & 0 & 0 & C_{55} & 0\\ 0 & 0 & 0 & 0 & C_{44}\end{matrix}\right\}\left\{\begin{matrix}\epsilon_{xx}\\ \epsilon_{yy}\\ \gamma_{xy}\\ \gamma_{xz}\\ \gamma_{yz}\end{matrix}\right\} \tag{16}$$

The C_{ij} are the plane-stress reduced elastic constants:

$$C_{11} = \frac{E}{1-\nu^2}, \quad C_{12} = \nu\frac{E}{1-\nu^2}, \quad C_{22} = \frac{E}{1-\nu^2}, \tag{17}$$

$$C_{44} = G, \quad C_{55} = G, \quad C_{66} = G \tag{18}$$

It is interesting to note that the use of shear-correction factors is not considered, as would be the case of the first-order shear deformation theory.

We consider virtual (mathematical) layers of constant thickness, each containing a homogeneized modulus of elasticity, E^k, and a homogeneized Poisson's ratio, ν^k. The functionally graded plate is divided into a NL layers of equal thickness. For each layer the volume fraction of the ceramic phase is defined as:

$$V_c^k = \left(0.5 + \frac{\tilde{z}}{h}\right)^p \tag{19}$$

where $\tilde{z}$ is the thickness coordinate of a point of each layer, and p is the polynomial gradation law exponent. The volume fraction for the metal phase is given as $V_m^k = 1 - V_c^k$.

For each virtual layer, the elastic properties E^k and ν^k can be computed in two ways. First, we consider the law-of-mistures:

$$E^k(z) = E_m V_m + E_c V_c; \quad \nu^k(z) = \nu_m V_m + \nu_c V_c \tag{20}$$

Second, we consider the Mori–Tanaka homogenization procedure [25,26]. In this homogenization method, we find the bulk modulus, K, and the effective shear modulus, G, of the composite equivalent layer as

$$\frac{K-K_m}{K_c-K_m}=\frac{V_c}{1+(1-V_c)\frac{K_c-K_m}{K_m+4/3G_m}};\quad \frac{G-G_m}{G_c-G_m}=\frac{V_c}{1+(1-V_c)\frac{G_c-G_m}{G_m+f_m}} \tag{21}$$

where

$$f_m=\frac{G_m(9K_m+8G_m)}{6(K_m+2G_m)} \tag{22}$$

The effective values of Young's modulus, E^k, and Poisson's ratio, v^k, are found from

$$E^k=\frac{9K^kG^k}{3K^k+G^k};\quad v^k=\frac{3K^k-2G^k}{2(3K^k+G^k)} \tag{23}$$

After using the law-of-mixtures or the Mori–Tanaka homogenization procedure, the computation of the elastic constants C_{ij}^k is performed for each layer based on v^k and E^k. For example,

$$C_{12}^k=\frac{E^k(v^k+(v^k)^2)}{1-3(v^k)^2-2(v^k)^3} \tag{24}$$

Other C_{ij}^k terms follow a similar procedure.

2.4. Governing equations

The equations of motion of the hyperbolic sine theory are derived from the Principle of Virtual Displacements (PVD). In analytical form, it can be stated as:

$$\int_\Omega\left\{\delta\boldsymbol{\epsilon}_p^T\boldsymbol{\sigma}_p+\delta\boldsymbol{\epsilon}_n^T\boldsymbol{\sigma}_n\right\}d\Omega=\int_\Omega\{\rho\,\delta\boldsymbol{u}^T\ddot{\boldsymbol{u}}+\delta\boldsymbol{u}^T\boldsymbol{p}\}d\Omega \tag{25}$$

where (p) indicates in-plane components (xx), (yy) and (xy), and (n) the transverse components (xz), (yz) and (zz). Ω is the volume of the plate, δ denotes a virtual variation and T indicates the transpose operator. ρ is the density of the material and double dots denote acceleration. $\boldsymbol{p}=\{p_x,p_y,p_z\}$ is the external load applied to the structure. For the considered functionally graded plate, the PVD can be written as:

$$\begin{aligned}&\sum_{k=1}^{NL}\int_{\Omega_k}\int_{A_k}\left(\delta\boldsymbol{\epsilon}_p^T\boldsymbol{\sigma}_p^k+\delta\boldsymbol{\epsilon}_n^T\boldsymbol{\sigma}_n^k\right)dz\,d\Omega_k\\&\quad=\sum_{k=1}^{NL}\int_{\Omega_k}\int_{A_k}(\rho^k\,\delta\boldsymbol{u}^T\ddot{\boldsymbol{u}}+\delta\boldsymbol{u}^T\boldsymbol{p})dz\,d\Omega_k\end{aligned} \tag{26}$$

where Ω_k is the in-plane integration domain (x,y) and A_k is the integration domains in z direction of the k-th layer. Integrating through the thickness and summing on the index k, integrating by parts with respect to x and y and collecting the coefficients of δu_0, δv_0, δw_0, δu_1, δv_1, δw_1, δu_Z, δv_Z, and δw_2, the following equations of motion are obtained:

$$\begin{aligned}\delta u_0:&\sum_{k=1}^{NL}\left(-\frac{\partial N_{xx}^k}{\partial x}-\frac{\partial N_{xy}^k}{\partial y}\right)\\&=\sum_{k=1}^{NL}\int_{A_k}\left\{\rho^k\left(\ddot{u}_0+z\ddot{u}_1+\sinh\left(\frac{\pi z}{h}\right)\ddot{u}_Z\right)+p_x\right\}dz\\\delta v_0:&\sum_{k=1}^{NL}\left(-\frac{\partial N_{xy}^k}{\partial x}-\frac{\partial N_{yy}^k}{\partial y}\right)\\&=\sum_{k=1}^{NL}\int_{A_k}\left\{\rho^k\left(\ddot{v}_0+z\ddot{v}_1+\sinh\left(\frac{\pi z}{h}\right)\ddot{v}_Z\right)+p_y\right\}dz\\\delta w_0:&\sum_{k=1}^{NL}\left(-\frac{\partial Q_{xz}^k}{\partial x}-\frac{\partial Q_{yz}^k}{\partial y}\right)\\&=\sum_{k=1}^{NL}\int_{A_k}\{\rho^k(\ddot{w}_0+z\ddot{w}_1+z^2\ddot{w}_2)+p_z\}dz\\\delta u_1:&\sum_{k=1}^{NL}\left(-\frac{\partial M_{xx}^k}{\partial x}-\frac{\partial M_{xy}^k}{\partial y}+Q_{xz}^k\right)\\&=\sum_{k=1}^{NL}\int_{A_k}\left\{\rho^kz\left(\ddot{u}_0+z\ddot{u}_1+\sinh\left(\frac{\pi z}{h}\right)\ddot{u}_Z\right)+zp_x\right\}dz\\\delta v_1:&\sum_{k=1}^{NL}\left(-\frac{\partial M_{xy}^k}{\partial x}-\frac{\partial M_{yy}^k}{\partial y}+Q_{yz}^k\right)\\&=\sum_{k=1}^{NL}\int_{A_k}\left\{\rho^kz\left(\ddot{v}_0+z\ddot{v}_1+\sinh\left(\frac{\pi z}{h}\right)\ddot{v}_Z\right)+zp_y\right\}dz\\\delta w_1:&\sum_{k=1}^{NL}\left(-\frac{\partial M_{xz}^k}{\partial x}-\frac{\partial M_{yz}^k}{\partial y}+Q_{zz}^k\right)\\&=\sum_{k=1}^{NL}\int_{A_k}\{\rho^kz(\ddot{w}_0+z\ddot{w}_1+z^2\ddot{w}_2)+zp_z\}dz\\\delta u_Z:&\sum_{k=1}^{NL}\left(-\frac{\partial R_{xx}^{kZ}}{\partial x}-\frac{\partial R_{xy}^{kZ}}{\partial y}+R_{xz}^{kZ}\right)\\&=\sum_{k=1}^{NL}\int_{A_k}\left\{\rho^k\sinh\left(\frac{\pi z}{h}\right)\left(\ddot{u}_0+z\ddot{u}_1+\sinh\left(\frac{\pi z}{h}\right)\ddot{u}_Z\right)+\sinh\left(\frac{\pi z}{h}\right)p_x\right\}dz\\\delta v_Z:&\sum_{k=1}^{NL}\left(-\frac{\partial R_{xy}^{kZ}}{\partial x}-\frac{\partial R_{yy}^{kZ}}{\partial y}+R_{yz}^{kZ}\right)\\&=\sum_{k=1}^{NL}\int_{A_k}\left\{\rho^k\sinh\left(\frac{\pi z}{h}\right)\left(\ddot{v}_0+z\ddot{v}_1+\sinh\left(\frac{\pi z}{h}\right)\ddot{v}_Z\right)+\sinh\left(\frac{\pi z}{h}\right)p_y\right\}dz\\\delta w_2:&\sum_{k=1}^{NL}\left(-\frac{\partial R_{xz}^{k2}}{\partial x}-\frac{\partial R_{yz}^{k2}}{\partial y}+2M_{zz}^k\right)\\&=\sum_{k=1}^{NL}\int_{A_k}\{\rho^kz^2(\ddot{w}_0+z\ddot{w}_1+z^2\ddot{w}_2)+z^2p_z\}dz\end{aligned} \tag{27}$$

The following stress resultants for each fictitious layer are considered:

$$\begin{Bmatrix}N_{xx}^k\\N_{yy}^k\\N_{xy}^k\end{Bmatrix}=\int_{A_k}\begin{Bmatrix}\sigma_{xx}^k\\\sigma_{yy}^k\\\tau_{xy}^k\end{Bmatrix}dz,\quad\begin{Bmatrix}Q_{xz}^k\\Q_{yz}^k\\Q_{zz}^k\end{Bmatrix}=\int_{A_k}\begin{Bmatrix}\tau_{xz}^k\\\tau_{yz}^k\\\sigma_{zz}^k\end{Bmatrix}dz \tag{28}$$

$$\begin{Bmatrix}M_{xx}^k\\M_{yy}^k\\M_{xy}^k\end{Bmatrix}=\int_{A_k}z\begin{Bmatrix}\sigma_{xx}^k\\\sigma_{yy}^k\\\tau_{xy}^k\end{Bmatrix}dz,\quad\begin{Bmatrix}M_{xz}^k\\M_{yz}^k\\M_{zz}^k\end{Bmatrix}=\int_{A_k}z\begin{Bmatrix}\tau_{xz}^k\\\tau_{yz}^k\\\sigma_{zz}^k\end{Bmatrix}dz \tag{29}$$

$$\begin{Bmatrix}R_{xx}^{kZ}\\R_{yy}^{kZ}\\R_{xy}^{kZ}\end{Bmatrix}=\int_{A_k}\sinh\left(\frac{\pi z}{h}\right)\begin{Bmatrix}\sigma_{xx}^k\\\sigma_{yy}^k\\\tau_{xy}^k\end{Bmatrix}dz,\quad\begin{Bmatrix}R_{xz}^{kZ}\\R_{yz}^{kZ}\end{Bmatrix}=\frac{\pi}{h}\int_{A_k}\cosh\left(\frac{\pi z}{h}\right)\begin{Bmatrix}\tau_{xz}^k\\\tau_{yz}^k\end{Bmatrix}dz \tag{30}$$

$$\begin{Bmatrix}R_{xz}^{k2}\\R_{yz}^{k2}\end{Bmatrix}=\int_{A_k}z^2\begin{Bmatrix}\tau_{xz}^k\\\tau_{yz}^k\end{Bmatrix}dz \tag{31}$$

The corresponding mechanical boundary conditions are defined as:

$$\begin{aligned}\delta u_0&:n_xN_{xx}^k+n_yN_{xy}^k=n_x\overline{N}_{xx}^k+n_y\overline{N}_{xy}^k\\\delta v_0&:n_xN_{xy}^k+n_yN_{yy}^k=n_x\overline{N}_{xy}^k+n_y\overline{N}_{yy}^k\\\delta w_0&:n_xQ_{xz}^k+n_yQ_{yz}^k=n_x\overline{Q}_{xz}^k+n_y\overline{Q}_{yz}^k\end{aligned}$$

$$\begin{aligned}
&\delta u_1 : n_x M^k_{xx} + n_y M^k_{xy} = n_x \overline{M}^k_{xx} + n_y \overline{M}^k_{xy}\\
&\delta v_1 : n_x M^k_{xy} + n_y M^k_{yy} = n_x \overline{M}^k_{xy} + n_y \overline{M}^k_{yy}\\
&\delta w_1 : n_x M^k_{xz} + n_y M^k_{yz} = n_x \overline{M}^k_{xz} + n_y \overline{M}^k_{yz}\\
&\delta u_Z : n_x R^{kZ}_{xx} + n_y R^{kZ}_{xy} = n_x \overline{R}^{kZ}_{xx} + n_y \overline{R}^{kZ}_{xy}\\
&\delta v_Z : n_x R^{kZ}_{xy} + n_y R^{kZ}_{yy} = n_x \overline{R}^{kZ}_{xy} + n_y \overline{R}^{kZ}_{yy}\\
&\delta w_2 : n_x R^{k2}_{xz} + n_y R^{k2}_{yz} = n_x \overline{R}^{k2}_{xz} + n_y \overline{R}^{k2}_{yz}
\end{aligned} \tag{32}$$

where (n_x, n_y) denotes the unit normal-to-boundary vector and over-lined terms are the imposed resultants.

2.5. Equations of motion and boundary conditions in terms of displacements

In order to discretize the equations of motion by radial basis functions, we present in the following the explicit terms of the equations of motion and the boundary conditions in terms of the generalized displacements. The following equations are derived considering that the plate is subjected to a transverse external load p_z applied at the top of the plate $z = h/2$.

$$\begin{aligned}
\delta u_0 : &-\left(G_{11}\frac{\partial^2 u_Z}{\partial x^2} + G_{66}\frac{\partial^2 u_Z}{\partial y^2}\right) - (G_{12}+G_{66})\frac{\partial^2 v_Z}{\partial x \partial y}\\
&-\left(A_{11}\frac{\partial^2 u_0}{\partial x^2} + A_{66}\frac{\partial^2 u_0}{\partial y^2}\right) - (A_{12}+A_{66})\frac{\partial^2 v_0}{\partial x \partial y}\\
&-\left(B_{11}\frac{\partial^2 u_1}{\partial x^2} + B_{66}\frac{\partial^2 u_1}{\partial y^2}\right) - (B_{12}+B_{66})\frac{\partial^2 v_1}{\partial x \partial y} - A_{13}\frac{\partial w_1}{\partial x} - 2B_{13}\frac{\partial w_2}{\partial x}\\
&= I_1 \ddot{u}_1 + I_0 \ddot{u}_0 + I_5 \ddot{u}_Z
\end{aligned} \tag{33}$$

$$\begin{aligned}
\delta u_1 : &\left(-D_{11}\frac{\partial^2 u_1}{\partial x^2} + A_{55}u_1 - D_{66}\frac{\partial^2 u_1}{\partial y^2}\right)\\
&+\left(H_{55}u_Z + N_{11}\frac{\partial^2 u_Z}{\partial x^2} + N_{66}\frac{\partial^2 u_Z}{\partial y^2}\right) + (N_{12}+N_{66})\frac{\partial^2 v_Z}{\partial x \partial y}\\
&-\left(B_{11}\frac{\partial^2 u_0}{\partial x^2} + B_{66}\frac{\partial^2 u_0}{\partial y^2}\right) - (B_{12}+B_{66})\frac{\partial^2 v_0}{\partial x \partial y}\\
&-(D_{12}+D_{66})\frac{\partial^2 v_1}{\partial x \partial y} + (B_{55}-B_{13})\frac{\partial w_1}{\partial x}\\
&+(D_{55}-2D_{13})\frac{\partial w_2}{\partial x} + A_{55}\frac{\partial w_0}{\partial x}\\
&= I_7 \ddot{u}_Z + I_1 \ddot{u}_0 + I_2 \ddot{u}_1
\end{aligned} \tag{34}$$

$$\begin{aligned}
\delta u_Z : &-\left(G_{11}\frac{\partial^2 u_0}{\partial x^2} + G_{66}\frac{\partial^2 u_0}{\partial y^2}\right) + (O_{55}-G_{55}-G_{13})\frac{\partial w_1}{\partial x}\\
&+\left(H_{55}u_1 + N_{11}\frac{\partial^2 u_1}{\partial x^2} + N_{66}\frac{\partial^2 u_1}{\partial y^2}\right) - (G_{12}+G_{66})\frac{\partial^2 v_0}{\partial x \partial y}\\
&+\left(-J_{11}\frac{\partial^2 u_Z}{\partial x^2} + R_{55}u_Z - J_{66}\frac{\partial^2 u_Z}{\partial y^2}\right) + (P_{55}+2N_{55}+2N_{13})\frac{\partial w_2}{\partial x}\\
&+(N_{12}+N_{66})\frac{\partial^2 v_1}{\partial x \partial y} - (J_{12}+J_{66})\frac{\partial^2 v_Z}{\partial x \partial y} + H_{55}\frac{\partial w_0}{\partial x}\\
&= I_7 \ddot{u}_1 + I_6 \ddot{u}_Z + I_5 \ddot{u}_0
\end{aligned} \tag{35}$$

$$\begin{aligned}
\delta v_0 : &-(G_{12}+G_{66})\frac{\partial^2 u_Z}{\partial x \partial y} - \left(G_{22}\frac{\partial^2 v_Z}{\partial y^2} + G_{66}\frac{\partial^2 v_Z}{\partial x^2}\right) - (A_{12}+A_{66})\frac{\partial^2 u_0}{\partial x \partial y}\\
&-\left(A_{22}\frac{\partial^2 v_0}{\partial y^2} + A_{66}\frac{\partial^2 v_0}{\partial x^2}\right) - (B_{12}+B_{66})\frac{\partial^2 u_1}{\partial x \partial y}\\
&-\left(B_{22}\frac{\partial^2 v_1}{\partial y^2} + B_{66}\frac{\partial^2 v_1}{\partial x^2}\right) - A_{23}\frac{\partial w_1}{\partial y} - 2B_{23}\frac{\partial w_2}{\partial y}\\
&= I_1 \ddot{v}_1 + I_0 \ddot{v}_0 + I_5 \ddot{v}_Z
\end{aligned} \tag{36}$$

$$\begin{aligned}
\delta v_1 : &\left(-D_{22}\frac{\partial^2 v_1}{\partial y^2} + A_{44}v_1 - D_{66}\frac{\partial^2 v_1}{\partial x^2}\right)\\
&+\left(H_{44}v_Z + N_{22}\frac{\partial^2 v_Z}{\partial y^2} + N_{66}\frac{\partial^2 v_Z}{\partial x^2}\right) + (N_{12}+N_{66})\frac{\partial^2 u_Z}{\partial x \partial y}\\
&-(B_{12}+B_{66})\frac{\partial^2 u_0}{\partial x \partial y} - (D_{12}+D_{66})\frac{\partial^2 u_1}{\partial x \partial y} - \left(B_{22}\frac{\partial^2 v_0}{\partial y^2} + B_{66}\frac{\partial^2 v_0}{\partial x^2}\right)\\
&+(B_{44}-B_{23})\frac{\partial w_1}{\partial y} + (D_{44}-2D_{23})\frac{\partial w_2}{\partial y} + A_{44}\frac{\partial w_0}{\partial y}\\
&= I_7 \ddot{v}_Z + I_1 \ddot{v}_0 + I_2 \ddot{v}_1
\end{aligned} \tag{37}$$

$$\begin{aligned}
\delta v_Z : &-(G_{12}+G_{66})\frac{\partial^2 u_0}{\partial x \partial y} + (O_{44}-G_{44}-G_{23})\frac{\partial w_1}{\partial y}\\
&+\left(H_{44}v_1 + N_{22}\frac{\partial^2 v_1}{\partial y^2} + N_{66}\frac{\partial^2 v_1}{\partial x^2}\right) - \left(G_{22}\frac{\partial^2 v_0}{\partial y^2} + G_{66}\frac{\partial^2 v_0}{\partial x^2}\right)\\
&+\left(-J_{22}\frac{\partial^2 v_Z}{\partial y^2} + R_{44}v_Z - J_{66}\frac{\partial^2 v_Z}{\partial x^2}\right) + (P_{44}+2N_{44}+2N_{23})\frac{\partial w_2}{\partial y}\\
&+(N_{12}+N_{66})\frac{\partial^2 u_1}{\partial x \partial y} - (J_{12}+J_{66})\frac{\partial^2 u_Z}{\partial x \partial y} + H_{44}\frac{\partial w_0}{\partial y}\\
&= I_7 \ddot{v}_1 + I_6 \ddot{v}_Z + I_5 \ddot{v}_0
\end{aligned} \tag{38}$$

$$\begin{aligned}
\delta w_0 : &-\left(A_{55}\frac{\partial^2 w_0}{\partial x^2} + A_{44}\frac{\partial^2 w_0}{\partial y^2}\right) - \left(B_{55}\frac{\partial^2 w_1}{\partial x^2} + B_{44}\frac{\partial^2 w_1}{\partial y^2}\right)\\
&-\left(D_{55}\frac{\partial^2 w_2}{\partial x^2} + D_{44}\frac{\partial^2 w_2}{\partial y^2}\right) - H_{55}\frac{\partial u_Z}{\partial x} - H_{44}\frac{\partial v_Z}{\partial y} - A_{55}\frac{\partial u_1}{\partial x}\\
&-A_{44}\frac{\partial v_1}{\partial y} + p_z\\
&= I_1 \ddot{w}_1 + I_2 \ddot{w}_2 + I_0 \ddot{w}_0
\end{aligned} \tag{39}$$

$$\begin{aligned}
\delta w_1 : &\left(-E_{55}\frac{\partial^2 w_2}{\partial x^2} + 2B_{33}w_2 - E_{44}\frac{\partial^2 w_2}{\partial y^2}\right) + (-O_{55}+G_{55}+G_{13})\frac{\partial u_Z}{\partial x}\\
&+(-O_{44}+G_{44}+G_{23})\frac{\partial v_Z}{\partial y} + \left(-D_{55}\frac{\partial^2 w_1}{\partial x^2} + A_{33}w_1 - D_{44}\frac{\partial^2 w_1}{\partial y^2}\right)\\
&+(B_{13}-B_{55})\frac{\partial u_1}{\partial x} + (B_{23}-B_{44})\frac{\partial v_1}{\partial y} - \left(B_{55}\frac{\partial^2 w_0}{\partial x^2} + B_{44}\frac{\partial^2 w_0}{\partial y^2}\right)\\
&+A_{13}\frac{\partial u_0}{\partial x} + A_{23}\frac{\partial v_0}{\partial y}\\
&= I_1 \ddot{w}_0 + I_2 \ddot{w}_1 + I_3 \ddot{w}_2
\end{aligned} \tag{40}$$

$$\begin{aligned}
\delta w_2 : &\left(-E_{55}\frac{\partial^2 w_1}{\partial x^2} + 2B_{33}w_1 - E_{44}\frac{\partial^2 w_1}{\partial y^2}\right)\\
&+\left(-F_{55}\frac{\partial^2 w_2}{\partial x^2} + 4D_{33}w_2 - F_{44}\frac{\partial^2 w_2}{\partial y^2}\right)\\
&-(P_{55}+2N_{55}+2N_{13})\frac{\partial u_Z}{\partial x} - (P_{44}+2N_{44}+2N_{23})\frac{\partial v_Z}{\partial y}\\
&+(2D_{13}-D_{55})\frac{\partial u_1}{\partial x} + (2D_{23}-D_{44})\frac{\partial v_1}{\partial y}\\
&-\left(D_{55}\frac{\partial^2 w_0}{\partial x^2} + D_{44}\frac{\partial^2 w_0}{\partial y^2}\right) + 2B_{13}\frac{\partial u_0}{\partial x} + 2B_{23}\frac{\partial v_0}{\partial y} + \left(\frac{h}{2}\right)^2 p_z\\
&= I_2 \ddot{w}_0 + I_3 \ddot{w}_1 + I_4 \ddot{w}_2
\end{aligned} \tag{41}$$

The laminate stiffness components can be computed as

$$
\begin{aligned}
A_{ij} &= \sum_{k=1}^{NL} c_{ij}^k (z_{k+1} - z_k); \quad B_{ij} = \frac{1}{2}\sum_{k=1}^{NL} c_{ij}^k (z_{k+1}^2 - z_k^2) \\
D_{ij} &= \frac{1}{3}\sum_{k=1}^{NL} c_{ij}^k (z_{k+1}^3 - z_k^3); \quad E_{ij} = \frac{1}{4}\sum_{k=1}^{NL} c_{ij}^k (z_{k+1}^4 - z_k^4) \\
F_{ij} &= \frac{1}{5}\sum_{k=1}^{NL} c_{ij}^k (z_{k+1}^5 - z_k^5) \\
G_{ij} &= \sum_{k=1}^{NL} c_{ij}^k \frac{h_k}{\pi}\left[\cosh\left(\frac{\pi z_{k+1}}{h_k}\right) - \cosh\left(\frac{\pi z_k}{h_k}\right)\right] \\
H_{ij} &= \sum_{k=1}^{NL} c_{ij}^k \left[\sinh\left(\frac{\pi z_{k+1}}{h_k}\right) - \sinh\left(\frac{\pi z_k}{h_k}\right)\right] \\
J_{ij} &= \sum_{k=1}^{NL} c_{ij}^k \left[\frac{h_k}{4\pi}\left[\sinh\left(\frac{2\pi z_{k+1}}{h_k}\right) - \sinh\left(\frac{2\pi z_k}{h_k}\right)\right] - \frac{1}{2}(z_{k+1} - z_k)\right] \\
N_{ij} &= \sum_{k=1}^{NL} c_{ij}^k \left[\left(\frac{h_k}{\pi}\right)^2 \left(\sinh\left(\frac{\pi z_{k+1}}{h_k}\right) - \sinh\left(\frac{\pi z_k}{h_k}\right)\right)\right. \\
&\quad \left. - \frac{h_k}{\pi}\left(z_{k+1}\cosh\left(\frac{\pi z_{k+1}}{h_k}\right) - z_k \cosh\left(\frac{\pi z_k}{h_k}\right)\right)\right] \\
O_{ij} &= \sum_{k=1}^{NL} c_{ij}^k \left[z_{k+1}\sinh\left(\frac{\pi z_{k+1}}{h_k}\right) - z_k \sinh\left(\frac{\pi z_k}{h_k}\right)\right] \\
P_{ij} &= \sum_{k=1}^{NL} c_{ij}^k \left[z_{k+1}^2\sinh\left(\frac{\pi z_{k+1}}{h_k}\right) - z_k^2 \sinh\left(\frac{\pi z_k}{h_k}\right)\right] \\
R_{ij} &= \sum_{k=1}^{NL} c_{ij}^k \left[\frac{\pi}{4h_k}\left[\sinh\left(\frac{2\pi z_{k+1}}{h_k}\right) - \sinh\left(\frac{2\pi z_k}{h_k}\right)\right]\right. \\
&\quad \left. + \frac{1}{2}\left(\frac{\pi}{h_k}\right)^2 (z_{k+1} - z_k)\right]
\end{aligned} \tag{42}
$$

The mass moments of inertia are defined by

$$
\begin{aligned}
I_0 &= \sum_{k=1}^{NL} \rho^k (z_{k+1} - z_k); \quad I_1 = \frac{1}{2}\sum_{k=1}^{NL} \rho^k (z_{k+1}^2 - z_k^2) \\
I_2 &= \frac{1}{3}\sum_{k=1}^{NL} \rho^k (z_{k+1}^3 - z_k^3); \quad I_3 = \frac{1}{4}\sum_{k=1}^{NL} \rho^k (z_{k+1}^4 - z_k^4) \\
I_4 &= \frac{1}{5}\sum_{k=1}^{NL} \rho^k (z_{k+1}^5 - z_k^5); \\
I_5 &= \sum_{k=1}^{NL} \rho^k \frac{h_k}{\pi}\left[\cosh\left(\frac{\pi z_{k+1}}{h_k}\right) - \cosh\left(\frac{\pi z_k}{h_k}\right)\right] \\
I_6 &= \sum_{k=1}^{NL} \rho^k \left[\frac{h_k}{4\pi}\left[\sin\left(\frac{2\pi z_{k+1}}{h_k}\right) - \sin\left(\frac{2\pi z_k}{h_k}\right)\right] - \frac{1}{2}(z_{k+1} - z_k)\right] \\
I_7 &= -\sum_{k=1}^{NL} \rho^k \left[\left(\frac{h_k}{\pi}\right)^2 \left(\sinh\left(\frac{\pi z_{k+1}}{h_k}\right) - \sinh\left(\frac{\pi z_k}{h_k}\right)\right)\right. \\
&\quad \left. - \frac{h_k}{\pi}\left(z_{k+1}\cosh\left(\frac{\pi z_{k+1}}{h_k}\right) - z_k \cosh\left(\frac{\pi z_k}{h_k}\right)\right)\right]
\end{aligned} \tag{43}
$$

where h_k is the thickness of each layer, z_k,z_{k+1} are the bottom and top z coordinate for each layer k, and ρ^k is the material density of the k-th layer.

2.5.1. Boundary conditions in terms of displacements

This meshless method based on collocation with radial basis functions needs the imposition of essential (e.g. $w = 0$) and mechanical (e.g. $M_{xx} = 0$) boundary conditions. Assuming a rectangular plate (for the sake of simplicity), Eq. (32) are expressed as follows: given the number of degrees of freedom, at each boundary point at edges $x = min$ or $x = max$ we impose

$$
\begin{aligned}
M_{xxu0} &= 2B_{13}w_2 + A_{13}w_1 + A_{11}\frac{\partial u_0}{\partial x} + A_{12}\frac{\partial v_0}{\partial y} + B_{11}\frac{\partial u_1}{\partial x} + B_{12}\frac{\partial v_1}{\partial y} \\
&\quad + G_{11}\frac{\partial u_Z}{\partial x} + G_{12}\frac{\partial v_Z}{\partial y}
\end{aligned} \tag{44}
$$

$$
\begin{aligned}
M_{xxu1} &= -N_{11}\frac{\partial u_Z}{\partial x} + 2D_{13}w_2 + B_{13}w_1 - N_{12}\frac{\partial v_Z}{\partial y} + B_{11}\frac{\partial u_0}{\partial x} \\
&\quad + D_{11}\frac{\partial u_1}{\partial x} + B_{12}\frac{\partial v_0}{\partial y} + D_{12}\frac{\partial v_1}{\partial y}
\end{aligned} \tag{45}
$$

$$
\begin{aligned}
M_{xxu2} &= -2N_{13}w_2 - N_{11}\frac{\partial u_1}{\partial x} - N_{12}\frac{\partial v_1}{\partial y} + J_{11}\frac{\partial u_Z}{\partial x} + J_{12}\frac{\partial v_Z}{\partial y} \\
&\quad + G_{13}w_1 + G_{11}\frac{\partial u_0}{\partial x} + G_{12}\frac{\partial v_0}{\partial y}
\end{aligned} \tag{46}
$$

$$
M_{xxv0} = A_{66}\frac{\partial u_0}{\partial y} + A_{66}\frac{\partial v_0}{\partial x} + B_{66}\frac{\partial u_1}{\partial y} + B_{66}\frac{\partial v_1}{\partial x} + G_{66}\frac{\partial u_Z}{\partial y} + G_{66}\frac{\partial v_Z}{\partial x} \tag{47}
$$

$$
M_{xxv1} = -N_{66}\frac{\partial u_Z}{\partial y} - N_{66}\frac{\partial v_Z}{\partial x} + B_{66}\frac{\partial u_0}{\partial y} + D_{66}\frac{\partial u_1}{\partial y} + B_{66}\frac{\partial v_0}{\partial x} + D_{66}\frac{\partial v_1}{\partial x} \tag{48}
$$

$$
M_{xxv2} = -N_{66}\frac{\partial u_1}{\partial y} - N_{66}\frac{\partial v_1}{\partial x} + J_{66}\frac{\partial u_Z}{\partial y} + J_{66}\frac{\partial v_Z}{\partial x} + G_{66}\frac{\partial u_0}{\partial y} + G_{66}\frac{\partial v_0}{\partial x} \tag{49}
$$

$$
M_{xxw0} = H_{55}u_Z + A_{55}u_1 + A_{55}\frac{\partial w_0}{\partial x} + B_{55}\frac{\partial w_1}{\partial x} + D_{55}\frac{\partial w_2}{\partial x} \tag{50}
$$

$$
M_{xxw1} = B_{55}u_1 + (O_{55} - G_{55})u_Z + B_{55}\frac{\partial w_0}{\partial x} + D_{55}\frac{\partial w_1}{\partial x} + E_{55}\frac{\partial w_2}{\partial x} \tag{51}
$$

$$
M_{xxw2} = D_{55}u_1 + (P_{55} + 2N_{55})u_Z + D_{55}\frac{\partial w_0}{\partial x} + E_{55}\frac{\partial w_1}{\partial x} + F_{55}\frac{\partial w_2}{\partial x} \tag{52}
$$

Similarly, given the number of degrees of freedom, at each boundary point at edges $y = min$ or $y = max$ we impose:

$$
M_{yyu0} = A_{66}\frac{\partial u_0}{\partial y} + A_{66}\frac{\partial v_0}{\partial x} + B_{66}\frac{\partial u_1}{\partial y} + B_{66}\frac{\partial v_1}{\partial x} + G_{66}\frac{\partial u_Z}{\partial y} + G_{66}\frac{\partial v_Z}{\partial x} \tag{53}
$$

$$
M_{yyu1} = -N_{66}\frac{\partial u_Z}{\partial y} - N_{66}\frac{\partial v_Z}{\partial x} + B_{66}\frac{\partial u_0}{\partial y} + D_{66}\frac{\partial u_1}{\partial y} + B_{66}\frac{\partial v_0}{\partial x} + D_{66}\frac{\partial v_1}{\partial x} \tag{54}
$$

$$
M_{yyu2} = -N_{66}\frac{\partial u_1}{\partial y} - N_{66}\frac{\partial v_1}{\partial x} + J_{66}\frac{\partial u_Z}{\partial y} + J_{66}\frac{\partial v_Z}{\partial x} + G_{66}\frac{\partial u_0}{\partial y} + G_{66}\frac{\partial v_0}{\partial x} \tag{55}
$$

$$
M_{yyv0} = A_{12}\frac{\partial u_0}{\partial x} + A_{22}\frac{\partial v_0}{\partial y} + B_{12}\frac{\partial u_1}{\partial x} + B_{22}\frac{\partial v_1}{\partial y} + G_{12}\frac{\partial u_Z}{\partial x} + G_{22}\frac{\partial v_Z}{\partial y} \tag{56}
$$

$$
M_{yyv1} = -N_{12}\frac{\partial u_Z}{\partial x} - N_{22}\frac{\partial v_Z}{\partial y} + B_{12}\frac{\partial u_0}{\partial x} + D_{12}\frac{\partial u_1}{\partial x} + B_{22}\frac{\partial v_0}{\partial y} + D_{22}\frac{\partial v_1}{\partial y} \tag{57}
$$

$$
M_{yyv2} = -N_{12}\frac{\partial u_1}{\partial x} - N_{22}\frac{\partial v_1}{\partial y} + J_{12}\frac{\partial u_Z}{\partial x} + J_{22}\frac{\partial v_Z}{\partial y} + G_{12}\frac{\partial u_0}{\partial x} + G_{22}\frac{\partial v_0}{\partial y} \tag{58}
$$

$$M_{yyw0} = H_{44}\,v_Z + A_{44}\,v_1 + A_{44}\frac{\partial w_0}{\partial y} + B_{44}\frac{\partial w_1}{\partial y} + D_{44}\frac{\partial w_2}{\partial y} \tag{59}$$

$$M_{yyw1} = B_{44}\,v_1 + (O_{44} - G_{44})\,v_Z + B_{44}\frac{\partial w_0}{\partial y} + D_{44}\frac{\partial w_1}{\partial y} + E_{44}\frac{\partial w_2}{\partial y} \tag{60}$$

$$M_{yyw2} = D_{44}\,v_1 + (P_{44} + 2N_{44})\,v_Z + D_{44}\frac{\partial w_0}{\partial y} + E_{44}\frac{\partial w_1}{\partial y} + F_{44}\frac{\partial w_2}{\partial y} \tag{61}$$

with A_{ij}, B_{ij}, D_{ij}, E_{ij}, F_{ij}, G_{ij}, H_{ij}, J_{ij}, N_{ij}, O_{ij}, P_{ij}, R_{ij} already described in (42).

3. The radial basis function method

For the sake of completeness we present here the basics of collocation with radial basis functions for static and vibrations problems.

3.1. The static problem

In this section the formulation of a global unsymmetrical collocation RBF-based method to compute elliptic operators is presented. Consider a linear elliptic partial differential operator L and a bounded region Ω in $\mathbb{R}^n$ with boundary $\partial\Omega$. In the static problems we seek the computation of displacements ($\mathbf{u}$) from the global system of equations

$$\mathcal{L}\mathbf{u} = \mathbf{f} \text{ in } \Omega; \quad \mathcal{L}_B\mathbf{u} = \mathbf{g} \text{ on } \partial\Omega \tag{62}$$

where $\mathcal{L}$, $\mathcal{L}_B$ are linear operators in the domain and on the boundary, respectively. The right-hand sides in (62) represent the external forces applied on the plate and the boundary conditions applied along the perimeter of the plate, respectively. The PDE problem defined in (62) will be replaced by a finite problem, defined by an algebraic system of equations, after the radial basis expansions.

3.2. The eigenproblem

The eigenproblem looks for eigenvalues (λ) and eigenvectors ($\mathbf{u}$) that satisfy

$$\mathcal{L}\mathbf{u} + \lambda\mathbf{u} = 0 \text{ in } \Omega; \quad \mathcal{L}_B\mathbf{u} = 0 \text{ on } \partial\Omega \tag{63}$$

As in the static problem, the eigenproblem defined in (63) is replaced by a finite-dimensional eigenvalue problem, based on RBF approximations.

3.3. Radial basis functions approximations

The radial basis function (ϕ) approximation of a function ($\mathbf{u}$) is given by

$$\tilde{\mathbf{u}}(\mathbf{x}) = \sum_{i=1}^{N} \alpha_i \phi(\|x - y_i\|_2), \quad \mathbf{x} \in \mathbb{R}^n \tag{64}$$

where y_i, $i = 1, \ldots, N$ is a finite set of distinct points (centers) in $\mathbb{R}^n$. Although we can use many RBFs, in this paper we restrict to the Wendland function, defined as

$$\phi(r) = (1 - c\,r)_+^8\left(32(c\,r)^3 + 25(c\,r)^2 + 8c\,r + 1\right) \tag{65}$$

where the Euclidian distance r is real and non-negative and c is a positive shape parameter. The shape parameter (c) was obtained by an optimization procedure, as detailed in Ferreira and Fasshauer [27].

Considering N distinct interpolations, and knowing $u(x_j)$, $j = 1, 2, \ldots, N$, we find α_i by the solution of a $N \times N$ linear system

$$\mathbf{A}\boldsymbol{\alpha} = \mathbf{u} \tag{66}$$

where $\mathbf{A} = [\phi(\|x - y_i\|_2)]_{N\times N}$, $\boldsymbol{\alpha} = [\alpha_1, \alpha_2, \ldots, \alpha_N]^T$ and $\mathbf{u} = [u(x_1), u(x_2), \ldots, u(x_N)]^T$.

3.4. Solution of the static problem

The solution of a static problem by radial basis functions considers N_I nodes in the domain and N_B nodes on the boundary, with a total number of nodes $N = N_I + N_B$. We denote the sampling points by $x_i \in \Omega$, $i = 1, \ldots, N_I$ and $x_i \in \partial\Omega$, $i = N_I + 1, \ldots, N$. At the points in the domain we solve the following system of equations

$$\sum_{i=1}^{N} \alpha_i \mathcal{L}\phi(\|x - y_i\|_2) = \mathbf{f}(x_j), \quad j = 1, 2, \ldots, N_I \tag{67}$$

or

$$\mathcal{L}^I\boldsymbol{\alpha} = \mathbf{F} \tag{68}$$

where

$$\mathcal{L}^I = [\mathcal{L}\phi(\|x - y_i\|_2)]_{N_I\times N} \tag{69}$$

At the points on the boundary, we impose boundary conditions as

$$\sum_{i=1}^{N} \alpha_i \mathcal{L}_B\phi(\|x - y_i\|_2) = \mathbf{g}(x_j), \quad j = N_I + 1, \ldots, N \tag{70}$$

or

$$\mathbf{B}\boldsymbol{\alpha} = \mathbf{G} \tag{71}$$

where

$$\mathbf{B} = \mathcal{L}_B\phi\left[\left(\|x_{N_I+1} - y_j\|_2\right)\right]_{N_B\times N}$$

Therefore, we can write a finite-dimensional static problem as

$$\begin{bmatrix} \mathcal{L}^I \\ \mathbf{B} \end{bmatrix}\boldsymbol{\alpha} = \begin{bmatrix} \mathbf{F} \\ \mathbf{G} \end{bmatrix} \tag{72}$$

By inverting the system (72), we obtain the vector $\boldsymbol{\alpha}$. We then obtain the solution $\mathbf{u}$ using the interpolation Eq. (64).

3.5. Solution of the eigenproblem

As in the solution of the static problem, we consider N_I nodes in the interior of the domain and N_B nodes on the boundary. For $x_i \in \Omega$, $i = 1, \ldots, N_I$, we define the eigenproblem as

$$\sum_{i=1}^{N} \alpha_i \mathcal{L}\phi(\|x - y_i\|_2) = \lambda\tilde{\mathbf{u}}(x_j), \quad j = 1, 2, \ldots, N_I \tag{73}$$

or

$$\mathcal{L}^I\boldsymbol{\alpha} = \lambda\tilde{\mathbf{u}}^I \tag{74}$$

where

$$\mathcal{L}^I = [\mathcal{L}\phi(\|x - y_i\|_2)]_{N_I\times N} \tag{75}$$

For $x_i \in \partial\Omega$, $i = N_I + 1, \ldots, N$, we enforce the boundary conditions as

$$\sum_{i=1}^{N} \alpha_i \mathcal{L}_B\phi(\|x - y_i\|_2) = 0, \quad j = N_I + 1, \ldots, N \tag{76}$$

or

$$\mathbf{B}\boldsymbol{\alpha} = 0 \tag{77}$$

Eqs. (74) and (77) can now be solved as a generalized eigenvalue problem

$$\begin{bmatrix} \mathcal{L}^I \\ \mathbf{B} \end{bmatrix} \boldsymbol{\alpha} = \lambda \begin{bmatrix} \mathbf{A}^I \\ \mathbf{0} \end{bmatrix} \boldsymbol{\alpha} \tag{78}$$

where

$$\mathbf{A}^I = \phi\left[\left(\|x_{N_I} - y_j\|_2\right)\right]_{N_I \times N}$$

3.6. Discretization of the equations of motion and boundary conditions

The radial basis collocation method follows a simple implementation procedure. Taking Eq. (72), we compute

$$\boldsymbol{\alpha} = \begin{bmatrix} L^I \\ \mathbf{B} \end{bmatrix}^{-1} \begin{bmatrix} \mathbf{F} \\ \mathbf{G} \end{bmatrix} \tag{79}$$

This $\boldsymbol{\alpha}$ vector is then used to obtain solution $\tilde{\mathbf{u}}$, by using (64). If derivatives of $\tilde{\mathbf{u}}$ are needed, such derivatives are computed as

$$\frac{\partial \tilde{\mathbf{u}}}{\partial x} = \sum_{j=1}^{N} \alpha_j \frac{\partial \phi_j}{\partial x}; \quad \frac{\partial^2 \tilde{\mathbf{u}}}{\partial x^2} = \sum_{j=1}^{N} \alpha_j \frac{\partial^2 \phi_j}{\partial x^2}, \text{ etc.} \tag{80}$$

In the present collocation approach, we need to impose essential and natural boundary conditions. Consider, for example, the condition $w_0 = 0$, on a simply supported or clamped edge. We enforce the conditions by interpolating as

$$w_0 = 0 \rightarrow \sum_{j=1}^{N} \alpha_j^{W_0} \phi_j = 0 \tag{81}$$

Other boundary conditions are interpolated in a similar way.

3.7. Free vibrations problems

For free vibration problems we set the external force to zero, and assume harmonic solution in terms of displacements u_0, u_1, u_Z, v_0, v_1, v_Z, w_0, w_1, w_2 as

$$\begin{aligned} &u_0 = U_0(w,y)e^{i\omega t}; \quad u_1 = U_1(w,y)e^{i\omega t}; \quad u_Z = U_Z(w,y)e^{i\omega t}; \\ &v_0 = V_0(w,y)e^{i\omega t}; \quad v_1 = V_1(w,y)e^{i\omega t}; \quad v_Z = V_Z(w,y)e^{i\omega t}; \\ &w_0 = W_0(w,y)e^{i\omega t}; \quad w_1 = W_1(w,y)e^{i\omega t}; \quad w_2 = W_2(w,y)e^{i\omega t} \end{aligned} \tag{82}$$

where ω is the frequency of natural vibration. Substituting the harmonic expansion into Eq. (78) in terms of the amplitudes U_0, U_1, U_Z, V_0, V_1, V_Z, W_0, W_1, W_2, we may obtain the natural frequencies and vibration modes for the plate problem, by solving the eigenproblem

$$\left[\mathcal{L} - \omega^2 \mathcal{G}\right]\mathbf{X} = \mathbf{0} \tag{83}$$

where $\mathcal{L}$ collects all stiffness terms and $\mathcal{G}$ collects all terms related to the inertial terms. In (83) $\mathbf{X}$ are the modes of vibration associated with the natural frequencies defined as ω.

4. Numerical examples

4.1. Bending problems

In the next examples we use the hyperbolic sine plate theory to analyse simply supported (SSSS) square (side lengths $a = b$) plates subjected to a bi-sinusoidal transverse mechanical load, of bi-sinusoidal load $p_z = \bar{p}_z sin(\frac{\pi x}{a}) sin(\frac{\pi y}{b})$ applied at the top plate surface, $z = h/2$, $\bar{p}_z = 1$. Three side-to-thickness ratios (a/h) are considered 4, 10 and 100.

We consider 91 mathematical layers, in order to model the continuous variation of properties across the thickness direction.[1] We consider a Wendland C6 radial function as in (65), and a Chebyshev grid (see [27] for details).

4.1.1. Isotropic functionally graded plate

In this example, an isotropic FGM square plate with a polynomial material law, as given by Zenkour [2] is considered. The plate is graded from aluminum (bottom surface) to alumina (top surface) materials. The following functional relationship is considered for modulus of elasticity $E(z)$ in the thickness direction (z) [2]:

$$E(z) = E_m + (E_c - E_m)\left(\frac{2z+h}{2h}\right)^p \tag{84}$$

where E_m = 70 GPa and E_c = 380 GPa are the corresponding modulus of elasticity of the metal and ceramic phases, respectively; p is the (positive number) volume fraction exponent. The Poisson's ratio is considered constant (ν = 0.3).

The transverse displacement and the normal stresses are computed in normalized form as

$$\begin{aligned} &\bar{u}_z = \frac{10h^3 E_c}{a^4 \bar{p}_z} u_z\left(\frac{a}{2}, \frac{b}{2}\right) \qquad \bar{\sigma}_{xx} = \frac{h}{a\bar{p}_z}\sigma_{xx}\left(\frac{a}{2}, \frac{b}{2}\right) \\ &\bar{\sigma}_{yy} = \frac{h}{a\bar{p}_z}\sigma_{yy}\left(\frac{a}{2}, \frac{b}{2}\right) \qquad \bar{\sigma}_{zz} = \sigma_{zz}\left(\frac{a}{2}, \frac{b}{2}\right) \end{aligned} \tag{85}$$

The shear stresses are normalized according to

$$\bar{\sigma}_{xy} = \frac{h}{a\bar{p}_z}\sigma_{xy}(0,0); \quad \bar{\sigma}_{xz} = \frac{h}{a\bar{p}_z}\sigma_{xz}\left(0, \frac{b}{2}\right); \quad \bar{\sigma}_{yz} = \frac{h}{a\bar{p}_z}\sigma_{yz}\left(\frac{a}{2}, 0\right) \tag{86}$$

$\left(\frac{a}{2}, \frac{b}{2}\right)$ is the center of the plate, $\left(0, \frac{b}{2}\right)$ and $\left(\frac{a}{2}, 0\right)$ are the midpoints of the sides, and (0,0) is the corner of the plate.

The present approach with $\epsilon_{zz} \neq 0$ is compared with analytical solutions by Carrera et al. [28], the classical plate theory (CLT), the first-order shear deformation theory (FSDT), a generalized shear deformation theory by Zenkour [2] (who considered $\epsilon_{zz} = 0$), and finite element solutions by Carrera et al. [9]. We consider Chebyschev grids with 13^2, 17^2 and 21^2 points. Three FGM configurations are considered by using different p exponents (p = 1,4,10). Thick (a/h = 4) down to thin (a/h = 100) plates are analysed. Normalized transverse displacements ($\bar{u}_z$) and normal stresses ($\bar{\sigma}_{xx}$) at the central point of the plate and selected thickness coordinate are shown in Table 1. Our approach presents very close results to those theories that consider thickness stretching, and clearly deviates from those theories that neglect ϵ_{zz}, in particular for thicker plates. The present approach presents very close results to Carrera's analytical solution [28].

In Figs. 1–6 we present the evolution of the displacement and stresses across the thickness direction for various values of the exponent p, using a 21^2 grid. As can be seen in Fig. 6, the transverse normal component σ_{zz} cannot be neglected for the present problem.

4.1.2. Sandwich square plate with FGM core

In this example we consider a sandwich plate with total thickness h, by using a polynomial material law for the core, as described in Zenkour [2]. The bottom skin is aluminium (E_m = 70 GPa) with thickness $h_b = 0.1h$ and the top skin is alumina (E_c = 380 GPa) with thickness $h_t = 0.1h$. The core is a FGM layer with the following functional relationship for modulus of elasticity $E(z)$ in the thickness direction z as in (84). The Poisson's ratio is considered constant ν = 0.3.

[1] A significant number of mathematical layers is needed to ensure correct computation of material properties at each thickness position.

Table 1
FGM isotropic plate with polynomial material law [2]. Effect of transverse normal strain ϵ_{zz} for a bending problem.

	a/h		$\bar{\sigma}_{xx}(h/3)$			$\bar{u}_z(0)$		
p		ϵ_{zz}	4	10	100	4	10	100
1	Ref. [28]	≠0	0.6221	1.5064	14.969	0.7171	0.5875	0.5625
	CLT	0	0.8060	2.0150	20.150	0.5623	0.5623	0.5623
	FSDT (k = 5/6)	0	0.8060	2.0150	20.150	0.7291	0.5889	0.5625
	GSDT [2]	0		1.4894			0.5889	
	Ref. [9] N = 4	0	0.7856	2.0068	20.149	0.7289	0.5890	0.5625
	Ref. [9] N = 4	≠0	0.6221	1.5064	14.969	0.7171	0.5875	0.5625
	Ref. [29]	≠0	0.5925	1.4945	14.969	0.6997	0.5845	0.5624
	Present 13^2 grid	≠0	0.5910	1.4911	14.873	0.7020	0.5868	0.5620
	Present 17^2 grid	≠0	0.5910	1.4916	14.930	0.7020	0.5868	0.5646
	Present 21^2 grid	≠0	0.5910	1.4917	14.944	0.7020	0.5868	0.5648
4	Ref. [28]	≠0	0.4877	1.1971	11.923	1.1585	0.8821	0.8286
	CLT	0	0.6420	1.6049	16.049	0.8281	0.8281	0.8281
	FSDT (k = 5/6)	0	0.6420	1.6049	16.049	1.1125	0.8736	0.828
	GSDT [2]	0		1.1783			0.8651	
	Ref. [9] N = 4	0	0.5986	1.5874	16.047	1.1673	0.8828	0.8286
	Ref. [9] N = 4	≠0	0.4877	1.1971	11.923	1.1585	0.8821	0.8286
	Ref. [29]	≠0	0.4404	1.1783	11.932	1.1178	0.8750	0.8286
	Present 13^2 grid	≠0	0.4341	1.1590	11.698	1.1094	0.8697	0.8205
	Present 17^2 grid	≠0	0.4340	1.1593	11.727	1.1095	0.8698	0.8238
	Present 21^2 grid	≠0	0.4340	1.1593	11.738	1.1095	0.8698	0.8241
10	Ref. [28]	≠0	0.3695	0.8965	8.9077	1.3745	1.0072	0.9361
	CLT	0	0.4796	1.1990	11.990	0.9354	0.9354	0.9354
	FSDT (k = 5/6)	0	0.4796	1.1990	11.990	1.3178	0.9966	0.9360
	GSDT [2]	0		0.8775			1.0089	
	Ref. [9] N = 4	0	0.4345	1.1807	11.989	1.3925	1.0090	0.9361
	Ref. [9] N = 4	≠0	0.1478	0.8965	8.9077	1.3745	1.0072	0.9361
	Ref. [29]	≠0	0.3227	1.1783	11.932	1.3490	0.8750	0.8286
	Present 13^2 grid	≠0	0.3108	0.8465	8.5844	1.3327	0.9886	0.9194
	Present 17^2 grid	≠0	0.3108	0.8467	8.5948	1.3327	0.9886	0.9225
	Present 21^2 grid	≠0	0.3108	0.8467	8.6013	1.3327	0.9886	0.9228

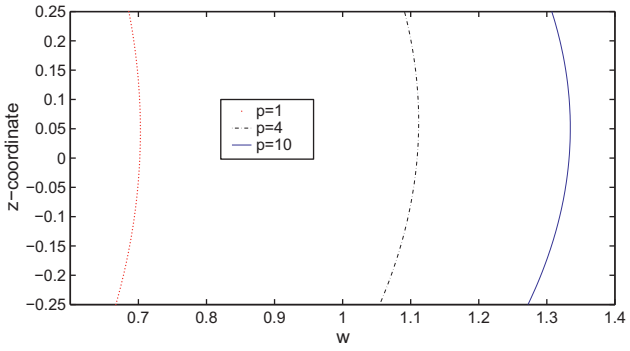

Fig. 1. FGM square plate subjected to sinusoidal load at the top, with $a/h = 4$. Displacement through the thickness direction for different values of p at the center of the plate $(\frac{a}{2}, \frac{b}{2})$ according to the hyperbolic sine theory.

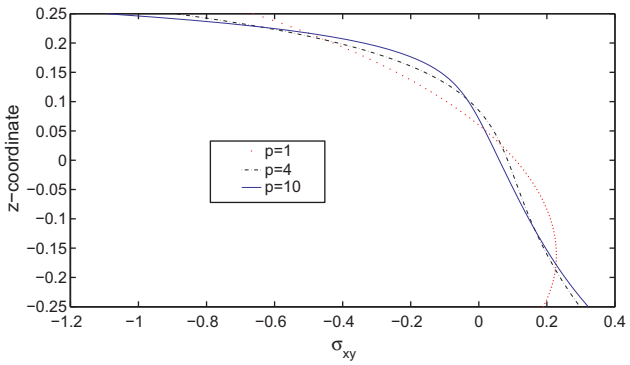

Fig. 3. FGM square plate subjected to sinusoidal load at the top, with $a/h = 4$. $\bar{\sigma}_{xy}$ through the thickness direction at the corner of the plate $(0,0)$ for different values of p according to the hyperbolic sine theory.

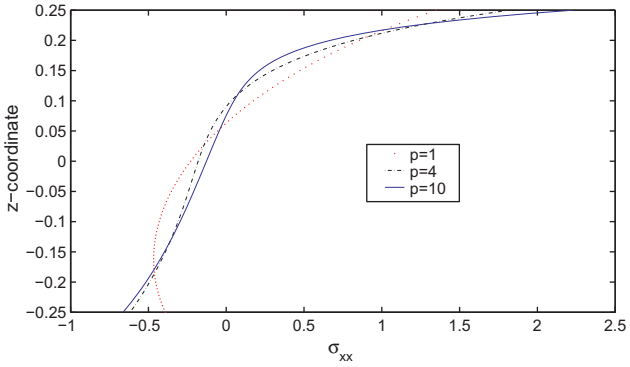

Fig. 2. FGM square plate subjected to sinusoidal load at the top, with $a/h = 4$. $\bar{\sigma}_{xx}$ through the thickness direction for different values of p at the center of the plate $(\frac{a}{2}, \frac{b}{2})$ according to the hyperbolic sine theory.

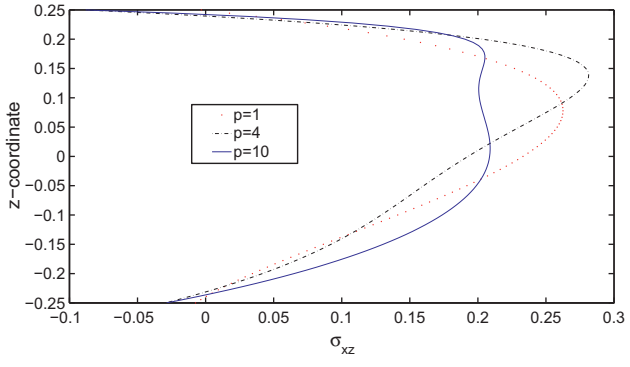

Fig. 4. FGM square plate subjected to sinusoidal load at the top, with $a/h = 4$. $\bar{\sigma}_{xz}$ through the thickness direction at the center of the plate $(0, \frac{b}{2})$ for different values of p according to the hyperbolic sine theory.

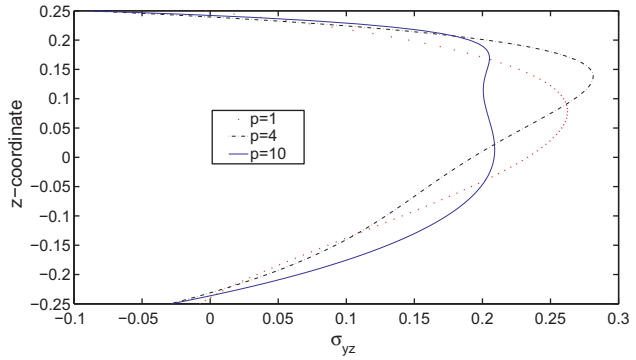

Fig. 5. FGM square plate subjected to sinusoidal load at the top, with $a/h = 4$. $\bar{\sigma}_{yz}$ through the thickness direction at the point $(\frac{a}{2}, 0)$ for different values of p according to the hyperbolic sine theory.

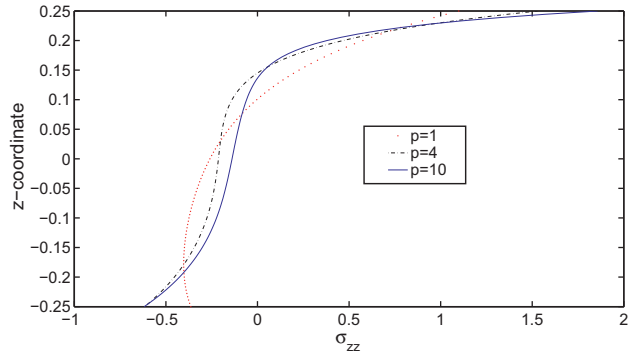

Fig. 6. FGM square plate subjected to sinusoidal load at the top, with $a/h = 4$. σ_{zz} through the thickness direction for different values of p at the center of the plate $(\frac{a}{2}, \frac{b}{2})$ according to the hyperbolic sine theory.

The same dimensionless forms as in (85) and (86) are used.

In Table 2 we present the normalized transverse displacement ($\bar{w}$) and the normalized transverse shear stress ($\bar{\sigma}_{xz}$) at selected locations. In Table 3 we present the normalized in-plane shear stress ($\bar{\sigma}_{xy}$) and the normalized transverse normal stress ($\bar{\sigma}_{zz}$) at selected locations. In both tables we consider three a/h ratios (4, 10 and 100), and three power-law exponents ($p = 1$, 4 and 10). We use a 21^2 Chebyshev grid and consider both $\epsilon_{zz} = 0$ and $\epsilon_{zz} \neq 0$ approaches. Our meshless results are compared in Table 2 with finite element results by Carrera et al. [9], and compare quite well for all cases. In Table 3 we compare the present approach with FEM results by Brischetto [30] and again the comparison is quite good.

In Figs. 7–13 we present the evolution of the displacement and stresses across the thickness direction for various values of the exponent p of a plate with side to thickness ratio $a/h = 10$, using a 21^2 grid.

The present numerical method presents very close results to those of Carrera et al. [9] for a $N = 4$ expansion.

The consideration of a non-zero ϵ_{zz} strain produces a significant change in the transverse displacement as well as in the normal stress. This becomes evident when we compare the present approch with that of Zenkour [2] who neglected the ϵ_{zz} strain in the formulation.

4.2. Free vibration problems

In this example, we study the free vibration behavior of simply-supported (SSSS) isotropic FGM Al/ZrO_2 plates. The modulus of elasticity are $E_m = 70$ GPa and $E_c = 380$ GPa, the mass densities are $\rho_m = 2702\ kg/m^3$ and $\rho_c = 5700\ kg/m^3$, and the Poisson's ratio is $\nu = 0.3$. We consider both the $\epsilon_{zz} = 0$ and the $\epsilon_{zz} \neq 0$ cases. We compare results with an exact (analytical) solution by Vel and Batra [31], and another meshless technique by Qian et al. [8]. In order to compare results, we use the Mori–Tanaka scheme for obtaining equivalent material properties.

In Table 4 we consider thin and thick plates, with $p = 1$, and using 21^2 Chebishev points. The ϵ_{zz} effect is significant. In fact, the exact solution by Vel and Batra [31] is achieved for all cases, by allowing $\epsilon_{zz} \neq 0$. In Table 5 we compare with the same sources, varying the p exponent, for $a/h = 5$ and using 21^2 points. Our present formulation with $\epsilon_{zz} \neq 0$ matches the exact solution.

In Fig. 14 the first four frequencies are presented for $p = 1$ and using 21^2 points. In Tables 6 and 7 we present the first ten frequencies for the same exponent p and compare results with those from Qian et al. [8] for different side-to-thickness ratios and different number of Chebishev points.

Table 2
Sandwich simply supported square plate with FGM core with polynomial material law [2] using a 21^2 grid. Effect of transverse normal strain ϵ_{zz} on σ_{xz} and transverse displacement for a bending problem using the hyperbolic sine theory.

	a/h		$\bar{\sigma}_{xz}(0, \frac{b}{2}, \frac{h}{3})$			$\bar{w}(0,0,0)$		
p		ϵ_{zz}	4	10	100	4	10	100
1	Ref. [9] $N = 4$	0	0.2604	0.2594	0.2593	0.7628	0.6324	0.6072
	Ref. [9] $N = 4$	$\neq 0$	0.2596	0.2593	0.2593	0.7735	0.6337	0.6072
	Ref. [29]	0	0.2703	0.2718	0.2720	0.7744	0.6356	0.6092
	Ref. [29]	$\neq 0$	0.2742	0.2788	0.2793	0.7416	0.6305	0.6092
	Present	0	0.2028	0.2017	0.2015	0.7744	0.6356	0.6093
	Present	$\neq 0$	0.2233	0.2271	0.2274	0.7417	0.6305	0.6093
4	Ref. [9] $N = 4$	0	0.2400	0.2398	0.2398	1.0930	0.8307	0.7797
	Ref. [9] $N = 4$	$\neq 0$	0.2400	0.2398	0.2398	1.0977	0.8308	0.7797
	Ref. [29]	0	0.2699	0.2726	0.2728	1.0847	0.8276	0.7785
	Ref. [29]	$\neq 0$	0.2723	0.2778	0.2785	1.0391	0.8202	0.7784
	Present	0	0.2813	0.2808	0.2806	1.0847	0.8276	0.7786
	Present	$\neq 0$	0.3154	0.3219	0.3230	1.0349	0.8195	0.7785
10	Ref. [9] $N = 4$	0	0.1932	0.1944	0.1946	1.2172	0.8740	0.8077
	Ref. [9] $N = 4$	$\neq 0$	0.1935	0.1944	0.1946	1.2240	0.8743	0.8077
	Ref. [29]	0	0.1998	0.2021	0.2022	1.2212	0.8718	0.8050
	Ref. [29]	$\neq 0$	0.2016	0.2059	0.2064	1.1780	0.8650	0.8050
	Present	0	0.2623	0.2624	0.2623	1.2212	0.8718	0.8051
	Present	$\neq 0$	0.2945	0.3000	0.3004	1.1720	0.8639	0.8050

Table 3
Sandwich simply supported square plate with FGM core with polynomial material law [2] using a 19^2 grid. Effect of transverse normal strain ϵ_{zz} on $\bar{\sigma}_{xy}$ and $\bar{\sigma}_{zz}$ for a bending problem $\bar{\sigma}_{zz} = \sigma_{zz}\frac{h}{ap_z}$.

	a/h		$\bar{\sigma}_{xy}(0,0,\frac{h}{3})$		$\bar{\sigma}_{zz}(\frac{a}{2},\frac{b}{2},0)$	
p		ϵ_{zz}	4	100	4	100
1	Ref. LD4 [30]	0	0.3007	8.4968	0.0922	0.0038
	Ref. LM4 [30]	≠0	0.3007	8.4968	0.0922	0.0038
	Ref. [29]	0	0.3303	8.4882	0.1276	3.1987
	Ref. [29]	≠0	0.3167	8.4911	0.0827	0.0034
	Present	0	0.3303	8.4903	0.1276	3.1983
	Present	≠0	0.3165	8.5056	0.0828	0.0034
5	Ref. LD4 [30]	0	0.1999	6.4942	0.0911	0.0037
	Ref. LM4 [30]	≠0	0.1996	6.4942	0.0924	0.0037
	Ref. [29]	0	0.2317	6.4454	0.0777	1.9535
	Ref. [29]	≠0	0.2248	6.4441	0.0522	0.0022
	Present	0	0.2317	6.4463	0.0777	1.9532
	Present	≠0	0.2247	6.4458	0.0522	0.0022
10	Ref. LD4 [30]	0	0.1412	5.1402	0.1064	0.0043
	Ref. LM4 [30]	≠0	0.1403	5.1401	0.1067	0.0042
	Ref. [29]	0	0.1745	5.0745	0.0685	1.6978
	Ref. [29]	≠0	0.1687	5.0754	0.0443	0.0018
	Present	0	0.1745	5.0752	0.0685	1.6975
	Present	≠0	0.1708	5.0784	0.0444	0.0018

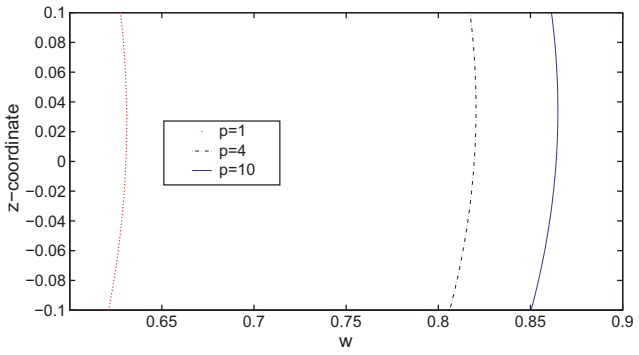

Fig. 7. Sandwich square plate with FGM core subjected to sinusoidal load at the top, with $a/h = 10$. Displacement through the thickness direction at the center of the plate $(\frac{a}{2},\frac{b}{2})$ for different values of p according to the hyperbolic sine theory.

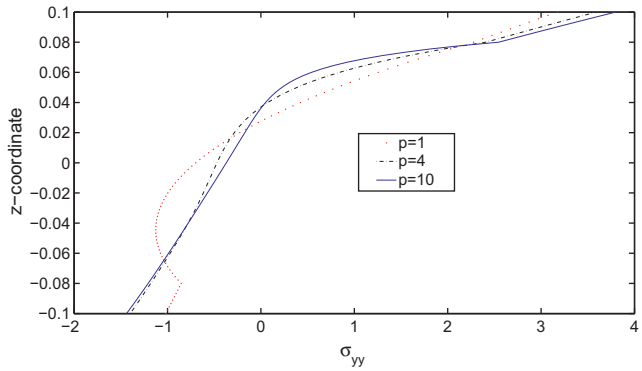

Fig. 9. Sandwich square plate with FGM core subjected to sinusoidal load at the top, with $a/h = 10$. $\bar{\sigma}_{yy}$ through the thickness direction at the center of the plate $(\frac{a}{2},\frac{b}{2})$ for different values of p according to the hyperbolic sine theory.

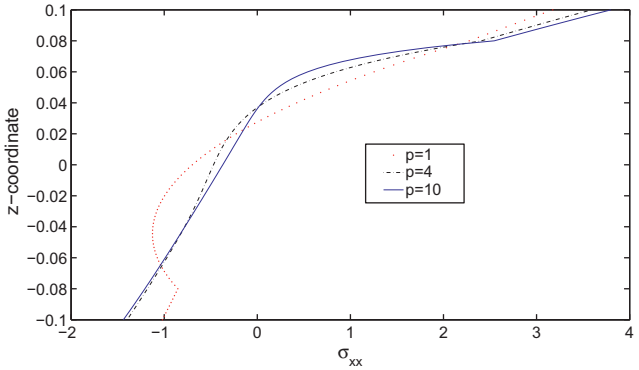

Fig. 8. Sandwich square plate with FGM core subjected to sinusoidal load at the top, with $a/h = 10$. $\bar{\sigma}_{xx}$ through the thickness direction at the center of the plate $(\frac{a}{2},\frac{b}{2})$ for different values of p according to the hyperbolic sine theory.

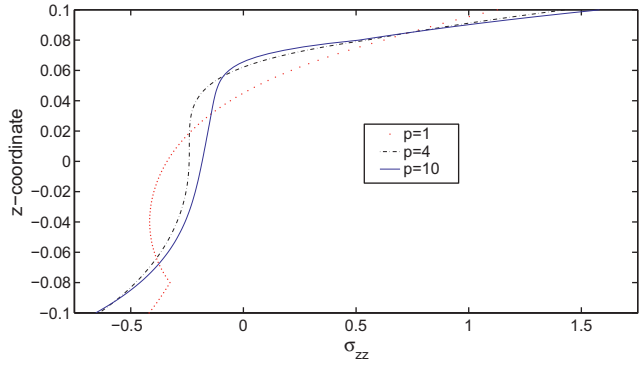

Fig. 10. Sandwich square plate with FGM core subjected to sinusoidal load at the top, with $a/h = 10$. σ_{zz} through the thickness direction at the center of the plate $(\frac{a}{2},\frac{b}{2})$ for different values of p according to the hyperbolic sine theory.

5. Conclusions

In this paper a new hyperbolic sine shear deformation theory accounting for through-the-thickness deformations was presented. Bending deformations and free vibrations of functionally graded plates were analysed. The equations of motion in terms of resultants and generalized displacements are obtained by the Carrera's Unified Formulation (CUF).

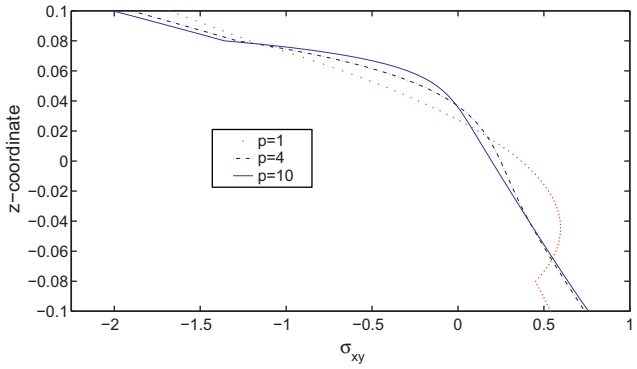

Fig. 11. Sandwich square plate with FGM core subjected to sinusoidal load at the top, with $a/h = 10$. $\bar{\sigma}_{xy}$ through the thickness direction at the point $(0,0)$ for different values of p according to the hyperbolic sine theory.

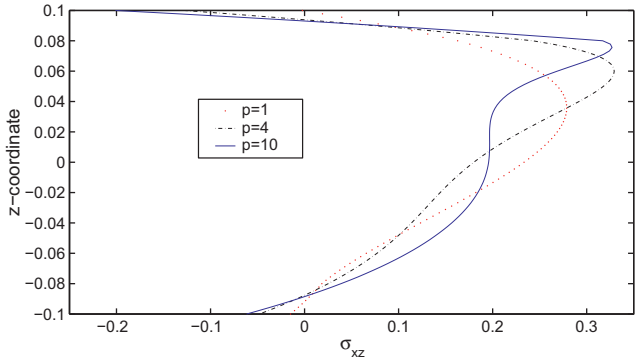

Fig. 12. Sandwich square plate with FGM core subjected to sinusoidal load at the top, with $a/h = 10$. $\bar{\sigma}_{xz}$ through the thickness direction at the point $(0,\frac{b}{2})$ for different values of p according to the hyperbolic sine theory.

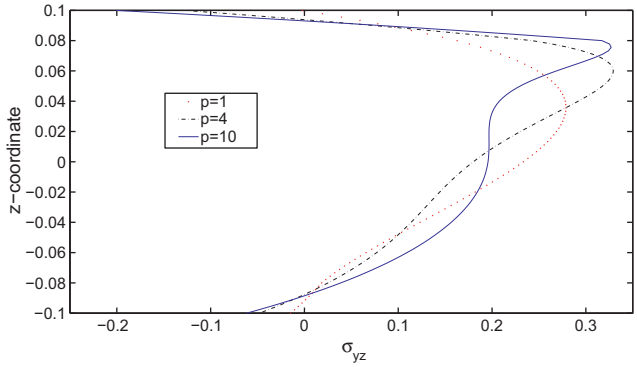

Fig. 13. Sandwich square plate with FGM core subjected to sinusoidal load at the top, with $a/h = 10$. $\bar{\sigma}_{yz}$ through the thickness direction at the point $(\frac{a}{2},0)$ for different values of p according to the hyperbolic sine theory.

Table 4
Fundamental frequency $\bar{\omega} = \omega h\sqrt{\rho_m/E_m}$ of a SSSS isotropic functionally graded plate (Al/ZrO_2), $p = 1$, using 21^2 points.

Source	a/h		
	20	10	5
Ref. [8]	0.0149	0.0584	0.2152
Exact [31]	0.0153	0.0596	0.2192
Ref. [29] ($\epsilon_{zz} = 0$)	0.0153	0.0595	0.2184
Ref. [29] ($\epsilon_{zz} \neq 0$)	0.0153	0.0596	0.2193
Present ($\epsilon_{zz} = 0$)	0.0153	0.0595	0.2184
Present ($\epsilon_{zz} \neq 0$)	0.0153	0.0596	0.2193

Table 5
Fundamental frequency $\bar{\omega} = \omega h\sqrt{\rho_m/E_m}$ of a SSSS isotropic functionally graded plate (Al/ZrO_2), $a/h = 5$, using 21^2 points and the hyperbolic sine theory.

Source	$p = 2$	$p = 3$	$p = 5$
Ref. [8]	0.2153	0.2172	0.2194
Exact [31]	0.2197	0.2211	0.2225
Ref. [29] ($\epsilon_{zz} = 0$)	0.2189	0.2202	0.2215
Ref. [29] ($\epsilon_{zz} \neq 0$)	0.2198	0.2212	0.2225
Present ($\epsilon_{zz} = 0$)	0.2191	0.2205	0.2220
Present ($\epsilon_{zz} \neq 0$)	0.2201	0.2216	0.2230

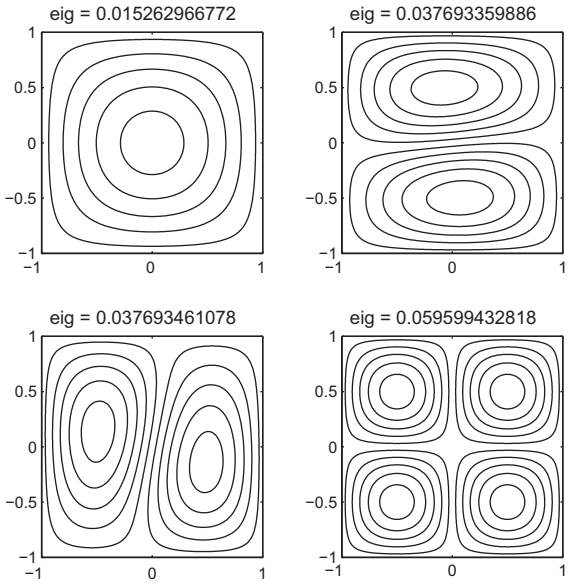

Fig. 14. First 4 frequencies $\bar{\omega} = \omega h\sqrt{\rho_m/E_m}$ of a SSSS isotropic functionally graded plate (Al/ZrO_2), with $a/h = 20$, $p = 1$, using 21^2 points and the hyperbolic sine theory.

Table 6
First 10 frequencies $\bar{\omega} = \omega h\sqrt{\rho_m/E_m}$ of a SSSS isotropic functionally graded plate (Al/ZrO_2), $p = 1$, $a/h = 20$, with the hyperbolic sine theory.

Present 13^2	17^2	21^2	Ref. [8]	Ref. [29]
0.0153	0.0153	0.0153	0.0149	0.0153
0.0377	0.0377	0.0377	0.0377	0.0377
0.0377	0.0377	0.0377	0.0377	0.0377
0.0596	0.0596	0.0596	0.0593	0.0596
0.0741	0.0739	0.0739	0.0747	0.0739
0.0741	0.0739	0.0739	0.0747	0.0739
0.0953	0.0950	0.0950	0.0769	0.0950
0.0953	0.0950	0.0950	0.0912	0.0950
0.1030	0.1030	0.1030	0.0913	0.1029
0.1030	0.1030	0.1030	0.1029	0.1029

Table 7
First 10 frequencies $\bar{\omega} = \omega h\sqrt{\rho_m/E_m}$ of a SSSS isotropic functionally graded plate (Al/ZrO_2), $p = 1$, $a/h = 10$, with the hyperbolic sine theory.

Present 13^2	17^2	21^2	Ref. [8]	Ref. [29]
0.0596	0.0596	0.0596	0.0584	0.0596
0.1426	0.1426	0.1426	0.1410	0.1426
0.1426	0.1426	0.1426	0.1410	0.1426
0.2059	0.2059	0.2059	0.2058	0.2058
0.2059	0.2059	0.2059	0.2058	0.2058
0.2194	0.2193	0.2193	0.2164	0.2193
0.2678	0.2676	0.2676	0.2646	0.2676
0.2678	0.2676	0.2676	0.2677	0.2676
0.2912	0.2912	0.2912	0.2913	0.2910
0.3367	0.3364	0.3364	0.3264	0.3363

Examples include an isotropic functionally graded plate and a sandwich plate with functionally graded core. Equations were interpolated by collocation with radial basis functions.

The present formulation produces highly accurate solutions for both bending deformations and free vibrations. The use of this hyperbolic sine theory and its meshless implementation are novel and serves to fill the gap of knowledge in this area.

Acknowledgment

The first author acknowledges support from FCT Grant SFRH/BD/45554/2008.

References

[1] Miyamoto Y, Kaysser WA, Rabin BH, Kawasaki A, Ford RG. Functionally graded materials: design, processing and applications. Kluwer Academic Publishers.; 1999.
[2] Zenkour AM. Generalized shear deformation theory for bending analysis of functionally graded plates. Appl Math Modell 2006;30.
[3] Cheng ZQ, Batra RC. Deflection relationships between the homogeneous kirchhoff plate theory and different functionally graded plate theories. Arch Mech 2000;52:143–58.
[4] Batra RC, Jin J. Natural frequencies of a functionally graded anisotropic rectangular plate. J Sound Vib 2005;282(1–2):509–16.
[5] Ferreira AJM, Batra RC, Roque CMC, Qian LF, Jorge RMN. Natural frequencies of functionally graded plates by a meshless method. Compos Struct 2006;75(1–4): 593–600.
[6] Reddy JN. Analysis of functionally graded plates. Int J Numer Methods Eng 2000;47:663–84.
[7] Ferreira AJM, Batra RC, Roque CMC, Qian LF, Martins PALS. Static analysis of functionally graded plates using third-order shear deformation theory and a meshless method. Compos Struct 2005;69(4):449–57.
[8] Qian LF, Batra RC, Chen LM. Static and dynamic deformations of thick functionally graded elastic plate by using higher-order shear and normal deformable plate theory and meshless local Petrov–Galerkin method. Composites: Part B 2004;35:685–97.
[9] Carrera E, Brischetto S, Cinefra M, Soave M. Effects of thickness stretching in functionally graded plates and shells. Compos Part B: Eng 2011;42:123–33.
[10] Kansa EJ. Multiquadrics – a scattered data approximation scheme with applications to computational fluid dynamics. Part i: surface approximations and partial derivative estimates. Comput Math Appl 1990;19(8/9):127–45.
[11] Ferreira AJM. A formulation of the multiquadric radial basis function method for the analysis of laminated composite plates. Compos Struct 2003;59: 385–92.
[12] Ferreira AJM. Thick composite beam analysis using a global meshless approximation based on radial basis functions. Mech Adv Mater Struct 2003; 10:271–84.
[13] Ferreira AJM, Roque CMC, Martins PALS. Analysis of composite plates using higher-order shear deformation theory and a finite point formulation based on the multiquadric radial basis function method. Composites: Part B 2003;34:627–36.
[14] Ferreira AJM, Roque CMC, Jorge RMN, Kansa EJ. Static deformations and vibration analysis of composite and sandwich plates using a layerwise theory and multiquadrics discretizations. Eng Anal Bound Elem 2005;29(12): 1104–14.
[15] Ferreira AJM, Roque CMC, Jorge RMN. Analysis of composite plates by trigonometric shear deformation theory and multiquadrics. Comput Struct 2005;83(27):2225–37.
[16] Ferreira AJM, Batra RC, Roque CMC, Qian LF, Jorge RMN. Natural frequencies of functionally graded plates by a meshless method. Compos Struct 2006; 75(1–4):593–600.
[17] Ferreira AJM, Roque CMC, Jorge RMN. Free vibration analysis of symmetric laminated composite plates by fsdt and radial basis functions. Comput Methods Appl Mech Eng 2005;194(39–41):4265–78.
[18] Ferreira AJM, Roque CMC, Martins PALS. Radial basis functions and higher-order shear deformation theories in the analysis of laminated composite beams and plates. Compos Struct 2004;66(1–4):287–93.
[19] Carrera E. C^0 Reissner–Mindlin multilayered plate elements including zig–zag and interlaminar stress continuity. Int J Numer Methods Eng 1996;39: 1797–820.
[20] Carrera E. Developments, ideas, and evaluations based upon Reissner's mixed variational theorem in the modelling of multilayered plates and shells. Appl Mech Rev 2001;54:301–29.
[21] Soldatos K. A transverse shear deformation theory for homogeneous monoclinic plates. Acta Mech 1992;94:195–220. doi:10.1007/BF01176650.
[22] Akavci S. Two new hyperbolic shear displacement models for orthotropic laminated composite plates. Mech Compos Mater 2010;46:215–26. doi:10.1007/s11029-010-9140-3.
[23] Akavci S, Tanrikulu A. Buckling and free vibration analyses of laminated composite plates by using two new hyperbolic shear-deformation theories. Mech Compos Mater 2008;44:145–54. doi:10.1007/s11029-008-9004-2.
[24] Meiche Noureddine El, Tounsi Abdelouahed, Ziane Noureddine, Mechab Ismail, Bedia El Abbes Adda. A new hyperbolic shear deformation theory for buckling and vibration of functionally graded sandwich plate. Int J Mech Sci 2011;53(4):237–47.
[25] Mori T, Tanaka K. Average stress in matrix and average elastic energy of materials with misfitting inclusions. Acta Metall 1973;21(5):571–4.
[26] Benveniste Y. A new approach to the application of Mori–Tanaka's theory in composite materials. Mech Mater 1987;6(2):147–57.
[27] Ferreira AJM, Fasshauer GE. Computation of natural frequencies of shear deformable beams and plates by a rbf-pseudospectral method. Comput Methods Appl Mech Eng 2006;196:134–46.
[28] Carrera E, Brischetto S, Robaldo A. Variable kinematic model for the analysis of functionally graded material plates. AIAA J 2008;46:194–203.
[29] Neves AMA, Ferreira AJM, Carrera E, Roque CMC, Cinefra M, Jorge RMN, Soares CMM. A quasi-3d sinusoidal shear deformation theory for the static and free vibration analysis of functionally graded plates. Composites Part B, in press.
[30] Brischetto S. Classical and mixed advanced models for sandwich plates embedding functionally graded cores. J Mech Mater Struct 2009;4: 13–33.
[31] Vel SS, Batra RC. Three-dimensional exact solution for the vibration of functionally graded rectangular plates. J Sound Vib 2004;272:703–30.